Self-Assembly

DOI: 10.1002/anie.200805010

Controllable Peptide–Dendron Self-Assembly: Interconversion of Nanotubes and Fibrillar Nanostructures**

*Hui Shao and Jon R. Parquette**

The programmed self-assembly of proteins into highly ordered nanostructures creates biomaterials displaying a wide range of physical properties often exceeding those of synthetic polymers.[1,2] The self-assembly of β-sheet-forming amphiphilic systems is thus emerging as a particularly powerful strategy to direct the self-assembly of relatively simple peptide building blocks toward sophisticated nanostructures.[3] Such peptide-based assemblers have shown significant potential in biomedical applications.[4] Many of these applications would benefit from an ability to extrinsically modulate the structure and properties of the assembly. Although strategies for designing β-sheet-forming peptides have been developed,[5] the nature of the ultimate superstructure (tape, ribbon, fibril, or tube) is determined by the hierarchical packing of the β-sheet blocks. Precise control of this level of assembly remains a significant challenge.[3,6]

Previously, we observed that peptide–dendron hybrids containing an intrinsically α-helical, alanine-rich sequence experienced an α-helix to β-sheet conformational transition going from 2,2,2-trifluoroethanol (TFE) to aqueous buffer.[7] Peptide–dendron hybrids having interdendron spacings of i, $i+6$, and i, $i+10$ adopted a β-sheet secondary structure in sodium phosphate butter (PBS) that further assembled into fibers, as shown by atomic force microscopy (AFM).[8] The presence of buffer salts attenuates electrostatic repulsions by screening the charges of the protonated lysine side chains, which promotes intermolecular aggregation into insoluble fibrillar networks.[9] Herein, we show that in pure water, the i, $i+10$ peptide–dendron hybrid (PDH) undergoes a transition from an amyloid-like fibrillar structure into soluble nanotubes. Further, the nanotube[10,11,14] structure and the amyloid-like fibrillar network can interconvert when the extent of charge repulsion is modulated through changes in pH value or in salt concentration (Figure 1). The assembly encapsulates Nile Red, a hydrophobic dye, in water with a capacity that is also modulated by changes in pH value.

Transmission electron microscopy (TEM) analysis of PDH in pure water revealed the formation of uniform nanotube aggregates. The nanotubes appear as two light, parallel lines separated by a dark center, consistent with the cross-sectional view of a hollow tubular structure filled with the negative stain, uranyl acetate (Figure 2a inset).[11] The nanotubes exhibit cross-sectional diameters of approximately 6 nm and persistence lengths on the order of several micrometers. Homogeneous elongated nanotubes were similarly observed by tapping-mode AFM (Figure 2b). AFM measurements along the long axis of the fibers revealed a constant height distribution indicating a relatively smooth nanotube

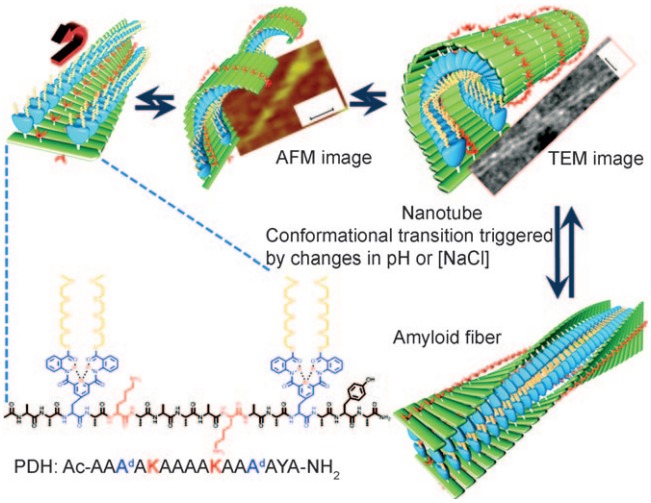

Figure 1. Schematic representation of nanotube and amyloid fiber formed by self-assembly of PDH. AFM image: A portion of the AFM image showing suprastructural undulations indicative of rolled-tape nanotube precursors (scale bar: 100 nm). TEM image: High-resolution image of a single nanotube (scale bar: 10 nm). A^d = dendron-substituted alanine.

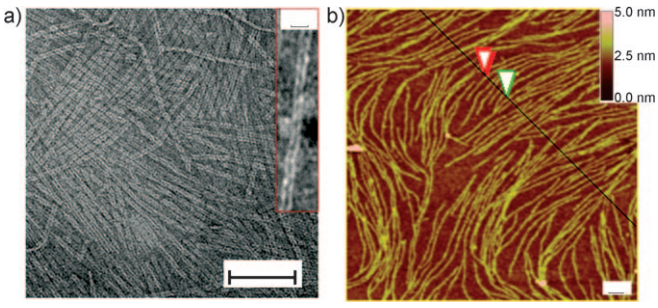

Figure 2. Self assembly of PDH into nanotubes in water (50 μM). a) TEM image of PDH (scale bar: 100 nm; carbon-coated copper grid). Uranyl acetate as negative stain. Inset: High-magnification TEM image of a single nanotube (scale bar: 10 nm). b) Tapping-mode AFM image on freshly cleaved mica (scale bar: 100 nm). See Supporting Information Figure S1 for detailed dimension analysis along the black line and at the colored arrows.

[*] H. Shao, Prof. J. R. Parquette
Department of Chemistry, The Ohio State University
100 W. 18th Ave. Columbus, OH 43210 (USA)
E-mail: parquett@chemistry.ohio-state.edu

[**] This work was supported by the National Science Foundation (CHE-0750004). We acknowledge the technical assistance and usage of the AFM core facility at DHLRI for this work.

Supporting information for this article is available on the WWW under http://dx.doi.org/10.1002/anie.200805010.

surface (Supporting Information, Figure S5). These observations are consistent with a dye-filled nanotube structure rather than pairs of twisted fibrils.[12] In contrast to most amyloid-type fibrillar aggregates, which often form insoluble networks,[6,13] the nanotubes align in nearly lamellar arrays and remain soluble in pure water at concentrations as high as 10 mg mL^{-1} without precipitating or gelation of the solvent. The soluble nature of the aggregates arises from repulsive electrostatic interactions between lysine residues, which are known to impede the intermolecular aggregation that leads to insoluble precipitates.[9] The 6 nm diameter of the nanotubes is among smallest β-sheet peptide nanotubes that have been observed.[14] A preliminary structural model consistent with the small diameter of the nanotubes could be envisioned by rolling the β-sheet over into a tube that sequesters the hydrophobic dendrons on the interior,[15] and projects one lysine on the surface as shown in Figure 1 (where lysine = K; red). Such superhelically rolled-tape intermediates would be observed as regular undulations in the height of the aggregates in contrast to the smooth surface of the more prevalent fully formed nanotubes.[15b] Accordingly, a few intermediate nanotube structures, albeit rare, could be distinguished in the AFM images, these structures exhibit regular variations in fiber height, consistent with an incompletely sealed, rolled-tape precursor to the nanotube structure. (Figure 1 and Supporting Information, Figure S4–5). This "rolled tape" assembly model resembles the folding of natural β-barrels,[16] synthetic dipeptide nanotubes,[11] and Aida and co-workers' graphitic nanotubes.[17]

The nanotube aggregates displayed exceptional stability. The β-sheet structure was apparent in the circular dichroism (CD) spectra, which showed a broad peak at 218 nm, at concentrations as low as 5 μM and at temperatures up to 90 °C (Supporting Information, Figure S2–3). In the deconvoluted FTIR spectra, a strong peak at 1621 cm^{-1} and a small peak at 1688 cm^{-1} indicated the presence of approximately 95% antiparallel β-sheet structure. The stability of the nanotubes is attributed to intermolecular hydrophobic[18] and π-stacking interactions[19] between the dendron side-chains.

Adjusting the proportion of the opposing electrostatic and hydrophobic interactions could be expected to modulate the structure of the aggregates. To screen the charge repulsion, the NaCl concentration was increased from 0 mM to 200 mM.[9,20] The CD spectra exhibited a steady reduction in the peak at 195 nm with increasing salt, indicating an alteration of the backbone twist of the β-sheet (Supporting Information, Figure S7).[21] Over time, at NaCl concentrations greater than 50 mM, white precipitates typical of amyloid fibrils were formed. TEM imaging indicated a gradual transition from nanotube to amyloid-type fibrillar structures as salt content was increased (Figure 3 a–c). In contrast to the nanotubes, the fibrils form an interwoven network (Figure 3 a, inset) commonly seen in amyloid-β fibers.[22]

Thioflavin T (ThT) binding studies are consistent with the increase in the proportion of amyloid fibers among the nanotubes at high salt concentration (Figure 3 d) as observed by TEM.[23] Amyloid formation can be monitored using ThT, which upon binding amyloid fibrils, experiences a strong increase in fluorescence emission intensity at 480 nm when excited at 450 nm. The nanotubes formed in pure water show relatively weak ThT emission at 480 nm. However, the intensity of emission at 482 nm increased significantly as NaCl was added, showing an abrupt increase at 200 mM NaCl, at which concentration a predominance of larger fibrillar bundles were observed by TEM (Figure 3 c). The weak binding of ThT by the nanotubes may be associated with an electrostatic repulsive interaction between the positively charged ThT and the charged nature of the lysines on the exterior surface of the nanotubes.[24] Although the addition of NaCl may increase ThT binding by screening this charge, the enhancement in ThT fluorescence correlates strongly with an increase in the proportion and size of amyloid-type fibrils in the TEM images (Figure 3 a–c).

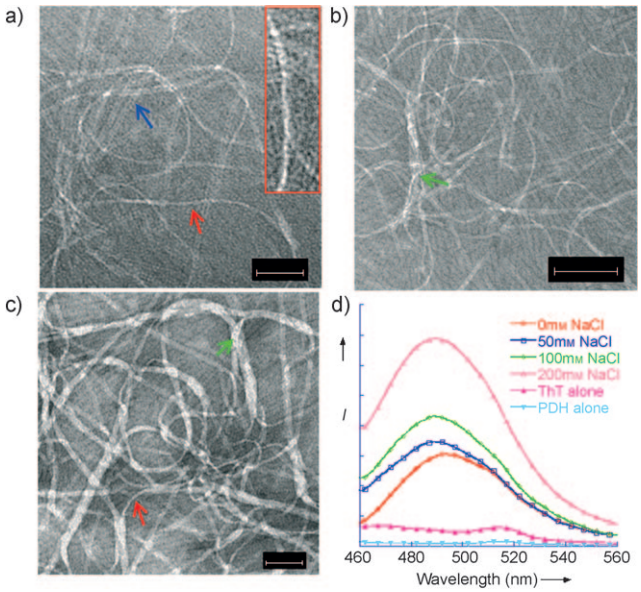

Figure 3. Effect of NaCl concentration on self-assembly of PDH (50 μM): transition from nanotubes to amyloid fibers. a) 50 mM NaCl, intertwining of two fibrils (inset), b) 100 mM NaCl, c) 200 mM NaCl. Blue arrows: nanotubes; red arrows: fibrils; green arrows: fibrillar bundles. All scale bars: 100 nm (carbon-coated copper grid). d) Fluorescence emission spectra of ThT (10 μM) in PDH water solutions (40 μM) with varying NaCl concentrations.

Adjusting the protonation state of the lysines with pH value also interconverts the nanotube and fibrillar structures. For example, at pH 1, the lysines would be charged and only nanotube structures are observed by TEM (Figure 4). Conversely, neutralization of the lysine side-chains at pH 11 produces a fibrillar network. Accordingly, the nanotubes and amyloid-β fibrils can be interconverted by adjusting the pH value or salt concentration.

Peptide-based aggregates capable of encapsulating hydrophobic molecules in water have significant potential to serve as vehicles for drug delivery.[4b] The structure of Aβ amyloid fibrils, based on solid-state NMR spectroscopic data, isolates hydrophobic interfaces on the interior the fibrillar aggregate.[15] The nanotube structure likewise sequesters the hydrophobic dendrons from the aqueous phase by positioning them within the tube. Based on the peak wavelength of 8-

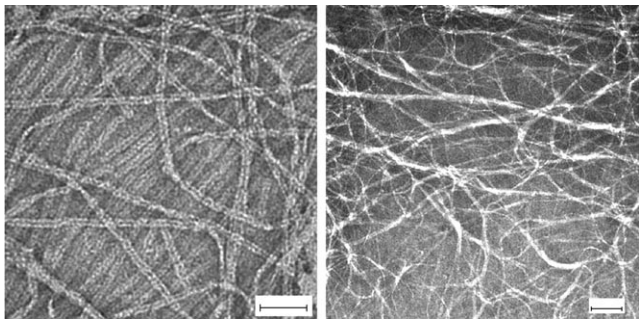

Figure 4. pH-dependence of self-assembly of PDH. TEM images of PDH (50 μM) on carbon-coated copper grid at pH 1 (left) and pH 11 (right). Transition from nanotube aggregates at pH 1 (scale bar: 50 nm) to a fibrillar network at pH 11 (scale bar: 100 nm).

anilino-1-naphthalenesulfonate (ANS; see Supporting Information Figure S9),[25] the polarity inside the PDH nanotubes and nanofibers corresponds to an E_T^N[26] of 0.72, between that of methanol ($E_T^N = 0.76$) and ethanol ($E_T^N = 0.65$).[27] Therefore, we recorded the amount of Nile Red encapsulated by PDH in water as a function of pH value.[28] Nile Red is a neutral, polarity-sensitive probe that is insoluble in water. PDH adopts a monomeric α-helical structure in 60% TFE/water. Consequently, in this solvent, Nile Red showed fluorescence emission at 650 nm, consistent with a hydrophilic environment (Figure 5a).[28] In contrast, the dye exhibited fluorescence at 618 nm in the presence of PDH in pure water, which indicates the presence of a hydrophobic environment around the dye. As shown in Figure 5b, the loading capacity of PDH progressively decreased going from pH 11 to 1.5. Notably, a significant reduction of the encapsulation efficiency transpired going from pH 7.4 to 5.5, the critical drop in pH value that occurs with endocytosis.[29] PDH encapsulated up to 16.1 and 7.2 mol% of Nile Red (relative to PDH) at pH 11 and pH 7.4, respectively (Supporting Information, Figure S10). The pH-dependent nanotube/fibril interconversion shown in Figure 4 suggests that the reduction in loading capacities were due to pH-induced changes in supramolecular structure.

We have shown that peptide–dendron hybrids interconvert between fibrillar and nanotube aggregates with changes in pH value or salt concentration. The hydrophobic interfaces created by the both PDH aggregates are capable of encapsulating hydrophobic molecules in water. Further, the loading capacity decreases when pH value decreases from 7.4 to 5.5, suggesting applications in drug delivery. We are currently exploring these potential applications in our laboratory.

Received: October 13, 2008
Revised: January 7, 2009
Published online: February 26, 2009

Keywords: dendrons · nanofibrils · nanotubes · peptides · self-assembly

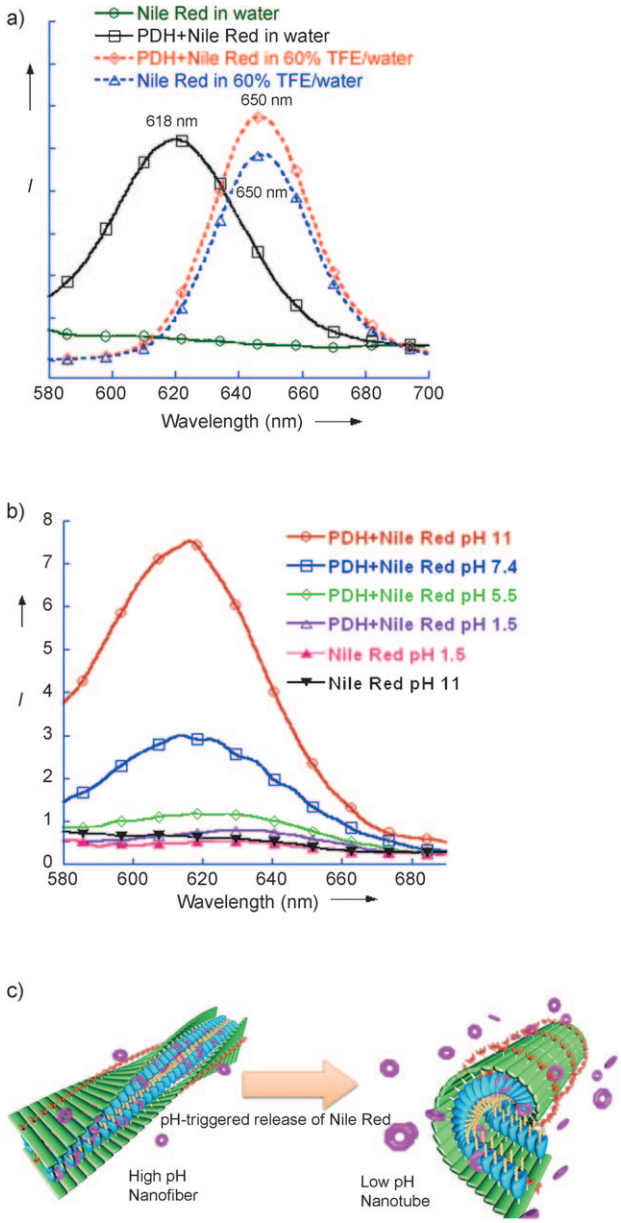

Figure 5. Encapsulation and release control experiments. a) Encapsulation: fluorescence emission spectra of Nile Red (80 μM) in PDH (50 μM) solutions. Water solution shown in solid lines and TFE/water (60%, v/v) shown in dashed lines. b) Release: fluorescence emission spectra of Nile Red (1 nmol) in PDH (12.5 nmol) solutions at varying pH value (excited at 550 nm). c) Schematic representation of pH-triggered release of Nile Red in PDH.

[1] *The Mechanical properties of biological materials*, Cambridge University Press, Cambridge, New York, **1980** (Published for the Society for Experimental Biology).
[2] T. P. Knowles, A. W. Fitzpatrick, S. Meehan, H. R. Mott, M. Vendruscolo, C. M. Dobson, M. E. Welland, *Science* **2007**, *318*, 1900–1903.
[3] a) R. V. Ulijn, A. M. Smith, *Chem. Soc. Rev.* **2008**, *37*, 664–675; I. Cherny, E. Gazit, *Angew. Chem.* **2008**, *120*, 4128–4136; *Angew. Chem. Int. Ed.* **2008**, *47*, 4062–4069; b) J. Hentschel, E. Krause, H. G. Boerner, *J. Am. Chem. Soc.* **2006**, *128*, 7722–7723; c) D. W. P. M. Löwik, J. C. M. van Hest, *Chem. Soc. Rev.* **2004**,

33, 234 – 245; d) D. Berti, *Curr. Opin. Colloid Interface Sci.* **2006**, *11*, 74 – 78; e) E. Kokkoli, A. Mardilovich, A. Wedekind, E. L. Rexeisen, A. Garg, J. A. Craig, *Soft Matter* **2006**, *2*, 1015 – 1024; f) S. E. Paramonov, H.-W. Jun, J. D. Hartgerink, *J. Am. Chem. Soc.* **2006**, *128*, 7291 – 7298; g) J. D. Hartgerink, E. Beniash, S. I. Stupp, *Science* **2001**, *294*, 1684 – 1688; h) T. S. Burkoth, T. L. S. Benzinger, D. N. M. Jones, K. Hallenga, S. C. Meredith, D. G. Lynn, *J. Am. Chem. Soc.* **1998**, *120*, 7655 – 7656.

[4] a) C. Stendahl, L.-J. Wang, L. W. Chow, D. B. Kaufman, S. I. Stupp, *Transplantation* **2008**, *86*, 478 – 481; b) Y.-b. Lim, E. Lee, M. Lee, *Angew. Chem.* **2007**, *119*, 3545 – 3548; *Angew. Chem. Int. Ed.* **2007**, *46*, 3475 – 3478; c) R. N. Mitra, D. Das, S. Roy, P. K. Das, *J. Phys. Chem. B* **2007**, *111*, 14107 – 14113; d) M. O. Guler, R. C. Claussen, S. I. Stupp, *J. Mater. Chem.* **2005**, *15*, 4507 – 4512; e) Okamoto, K. Takeda, *J. Drug Delivery Sci. Technol.* **2005**, *15*, 97 – 107.

[5] a) X. Zhao, S. Zhang, *Chem. Soc. Rev.* **2006**, *35*, 1105 – 1110; b) H. Yokoi, T. Kinoshita, S. Zhang, *Proc. Natl. Acad. Sci. USA* **2005**, *102*, 8414 – 8419.

[6] A. Aggeli, I. A. Nyrkova, M. Bell, R. Harding, L. Carrick, T. C. B. McLeish, A. N. Semenov, N. Boden, *Proc. Natl. Acad. Sci. USA* **2001**, *98*, 11857 – 11862.

[7] H. Shao, J. W. Lockman, J. R. Parquette, *J. Am. Chem. Soc.* **2007**, *129*, 1884 – 1885.

[8] For examples of a self-assembled peptide dendrimers see: a) V. Percec, M. Peterca, A. E. Dulcey, M. R. Imam, S. D. Hudson, S. Nummelin, P. Adelman, P. A. Heiney, *J. Am. Chem. Soc.* **2008**, *130*, 13079 – 13094; b) M. S. Kaucher, M. Peterca, A. E. Dulcey, A. J. Kim, S. A. Vinogradov, D. A. Hammer, P. A. Heiney, V. Percec, *J. Am. Chem. Soc.* **2007**, *129*, 11698 – 11699; c) V. A. R. Hirst, B. Huang, V. Castelletto, I. W. Hamley, D. K. Smith, *Chem. Eur. J.* **2007**, *13*, 2180 – 2188.

[9] H. Dong, S. E. Paramonov, L. Aulisa, E. L. Bakota, J. D. Hartgerink, *J. Am. Chem. Soc.* **2007**, *129*, 12468 – 12472.

[10] a) M. J. Krysmann, V. Castelletto, J. E. McKendrick, L. A. Clifton, I. W. Hamley, P. J. F. Harris, S. M. King, *Langmuir* **2008**, *24*, 8158 – 8162; b) K. Lu, J. Jacob, P. Thiyagarajan, V. P. Conticello, D. G. Lynn, *J. Am. Chem. Soc.* **2003**, *125*, 6391 – 6393; c) S. Vauthey, S. Santoso, H. Gong, N. Watson, S. Zhang, *Proc. Natl. Acad. Sci. USA* **2002**, *99*, 5355 – 5360; d) M. R. Ghadiri, J. R. Granja, R. A. Milligan, D. E. McRee, N. Khazanovich, *Nature* **1993**, *366*, 324 – 327; e) Y. Kim, M. F. Mayer, S. C. Zimmerman, *Angew. Chem.* **2003**, *115*, 1153 – 1158; *Angew. Chem. Int. Ed.* **2003**, *42*, 1121 – 1126.

[11] For similar TEM images of peptide nanotubes, see: a) M. Reches, E. Gazit, *Science* **2003**, *300*, 625 – 627; b) S. Matsumura, S. Uemura, H. Mihara, *Mol. BioSyst.* **2005**, *1*, 146 – 148; c) U. Raviv, D. J. Needleman, K. K. Ewert, C. R. Safinya, *J. Appl. Crystallogr.* **2007**, *40*, s83 – s87; d) S. Guha, M. G. B. Drew, A. Banerjee, *Chem. Mater.* **2008**, *20*, 2282 – 2290.

[12] For TEM/AFM of twisted fibrils, see: a) M. Zhu, P. O. Souillac, C. Ionescu-Zanetti, S. A. Carter, A. L. Fink, *J. Biol. Chem.* **2002**, *277*, 50914 – 50922; b) M. Dong, M. B. Hovgaard, S. Xu, D. E. Otzen, F. Besenbacher, *Nanotechnology* **2006**, *17*, 4003 – 4009; c) R. Tycko, *Biochemistry* **2003**, *42*, 3151 – 3159.

[13] T. Lûhrs, C. Ritter, M. Adrian, D. Riek-Loher, B. Bohrmann, H. Döbeli, D. Schubert, R. Riek, *Proc. Natl. Acad. Sci. USA* **2005**, *102*, 17342 – 17347.

[14] C. Valéry, M. Paternostre, B. Robert, T. Gulik-Krzywicki, T. Narayanan, J-C. Dedieu, G. Keller, M-L. Torres, R. Cherif-Cheikh, P. Calvo, F. Artzner, *Proc. Natl. Acad. Sci. USA* **2003**, *100*, 10258 – 10262.

[15] a) R. Tycko, *Q. Rev. Biophys.* **2006**, *39*, 1 – 55; b) K. Lu, J. Jacob, P. Thiyagarajan, V. P. Conticello, D. G. Lynn, *J. Am. Chem. Soc.* **2003**, *125*, 6391 – 6393.

[16] M. Faller, M. Niederweis, G. E. Schulz, *Science* **2004**, *303*, 1189 – 1192.

[17] J. P. Hill, W. Jin, A. Kosaka, T. Fukushima, H. Ichihara, T. Shimomura, K. Ito. T. Hashizume, N. Ishii, T. Aida, *Science* **2004**, *304*, 1481 – 1483.

[18] a) F. A. Syud, H. E. Stanger, S. H. Gellman, *J. Am. Chem. Soc.* **2001**, *123*, 8667 – 8677; b) W. Kim, M. H. Hecht, *Proc. Natl. Acad. Sci. USA* **2006**, *103*, 15824 – 15829.

[19] E. Gazit, *FASEB J.* **2002**, *16*, 77 – 83.

[20] K. Lu, L. Guo, A. K. Mehta, W. S. Childers, S. N. Dublin, S. Skanthakumar, V. P. Conticello, P. Thiyagarajan, R. P. Apkarian, D. G. Lynn, *Chem. Commun.* **2007**, 2729 – 2731.

[21] D. Sharma, S. Sharma, S. Pasha, S. K. Brahmachari, *FEBS Lett.* **1999**, *456*, 181 – 185.

[22] R. Khurana, C. Ionescu-Zanetti, M. Pope, J. Li, L. Nielson, M. Ramirez-Alvarado, L. Regan, A. L. Fink, S. A. Carter, *Biophys. J.* **2003**, *85*, 1135 – 1144.

[23] R. Khurana, C. Coleman, C. Ionescu-Zanetti, S. A. Carter, V. Krishna, R. K. Grover, R. Roy, S. Singh, *J. Struct. Biol.* **2005**, *151*, 229 – 238.

[24] R. Sabate, I. Lascu, S. J. Saupe, *J. Struct. Biol.* **2008**, *162*, 387 – 396.

[25] O. Hayashida, K. Ono, Y. Hisaeda, Y. Murakami, *Tetrahedron* **1995**, *51*, 8423 – 8436.

[26] E_T^N represents a normalized polarity scale. Values of E_T^N range from 0.0 (tetramethylsilane) to 1.0 (water). O. Hayashida, K. Ono, Y. Hisaeda, Y. Murakami, *Tetrahedron* **1995**, *51*, 8423 – 8436.

[27] J. Torrent, M. T. Alvarez-Martinez, M.-C. Harricane, F. Heitz, J.-P. Liautard, C. Balny, R. Lange, *Biochemistry* **2004**, *43*, 7162 – 7170.

[28] A. P. Goodwin, J. L. Mynar, Y. Ma, G. R. Fleming, J. M. J. Fréchet, *J. Am. Chem. Soc.* **2005**, *127*, 9952 – 9953.

[29] R. Haag, F. Kratz, *Angew. Chem.* **2006**, *118*, 1218 – 1237; *Angew. Chem. Int. Ed.* **2006**, *45*, 1198 – 1215.

